IEEE SA
STANDARDS ASSOCIATION

IEEE SA WHITE PAPER

MILLIMETER-WAVE MASSIVE MIMO DISTANCE STUDY

DISCUSSION ON MEASUREMENT TEST DISTANCE FOR DETERMINING EIRP OR TRP FOR ACTIVE ANTENNA SYSTEMS

Authored by

American National Standards Committee C63®

IEEE

TRADEMARKS AND DISCLAIMERS

IEEE believes the information in this publication is accurate as of its publication date; such information is subject to change without notice. IEEE is not responsible for any inadvertent errors.

The ideas and proposals in this specification are the respective author's views and do not represent the views of the affiliated organization.

ACKNOWLEDGMENTS

Special thanks are given to the following reviewers of this paper:

Dave Case, *Chair*
Benoit Derat, *Vice-Chair*
Jerry Ramie, *Secretary*

Nicholas Abbondante
Aurelian Bria
David Chamberlain
Jason Coder
Bob DeLisi
Jonas Fridén
William Graff
Michael Heckrotte
Steve Jones
Grace Lin
Jason Nixon
Robert Paxman
Aidin Razavi
Pelin Salem
Denys Shumakov
Mark Terrien

The Institute of Electrical and Electronics Engineers, Inc. 3 Park Avenue, New York, NY 10016-5997, USA

PDF: STDVA26741 979-8-8557-0474-7

NOTICE AND DISCLAIMER OF LIABILITY CONCERNING THE USE OF IEEE SA DOCUMENTS

This IEEE Standards Association ("IEEE SA") publication ("Work") is not a consensus standard document. Specifically, this document is NOT AN IEEE STANDARD. Information contained in this Work has been created by, or obtained from, sources believed to be reliable, and reviewed by members of the activity that produced this Work. IEEE and the C63 Committee expressly disclaim all warranties (express, implied, and statutory) related to this Work, including, but not limited to, the warranties of: merchantability; fitness for a particular purpose; non-infringement; quality, accuracy, effectiveness, currency, or completeness of the Work or content within the Work. In addition, IEEE and the C63 Committee disclaim any and all conditions relating to: results; and workmanlike effort. This document is supplied "AS IS" and "WITH ALL FAULTS."

Although the C63 Committee members who have created this Work believe that the information and guidance given in this Work serve as an enhancement to users, all persons must rely upon their own skill and judgment when making use of it. IN NO EVENT SHALL IEEE SA OR C63 Committee MEMBERS BE LIABLE FOR ANY ERRORS OR OMISSIONS OR DIRECT, INDIRECT, INCIDENTAL, SPECIAL, EXEMPLARY, OR CONSEQUENTIAL DAMAGES (INCLUDING, BUT NOT LIMITED TO: PROCUREMENT OF SUBSTITUTE GOODS OR SERVICES; LOSS OF USE, DATA, OR PROFITS; OR BUSINESS INTERRUPTION) HOWEVER CAUSED AND ON ANY THEORY OF LIABILITY, WHETHER IN CONTRACT, STRICT LIABILITY, OR TORT (INCLUDING NEGLIGENCE OR OTHERWISE) ARISING IN ANY WAY OUT OF THE USE OF THIS WORK, EVEN IF ADVISED OF THE POSSIBILITY OF SUCH DAMAGE AND REGARDLESS OF WHETHER SUCH DAMAGE WAS FORESEEABLE.

Further, information contained in this Work may be protected by intellectual property rights held by third parties or organizations, and the use of this information may require the user to negotiate with any such rights holders in order to legally acquire the rights to do so, and such rights holders may refuse to grant such rights. Attention is also called to the possibility that implementation of any or all of this Work may require use of subject matter covered by patent rights. By publication of this Work, no position is taken by the IEEE with respect to the existence or validity of any patent rights in connection therewith. The IEEE is not responsible for identifying patent rights for which a license may be required, or for conducting inquiries into the legal validity or scope of patents claims. Users are expressly advised that determination of the validity of any patent rights, and the risk of infringement of such rights, is entirely their own responsibility. No commitment to grant licenses under patent rights on a reasonable or non-discriminatory basis has been sought or received from any rights holder.

This Work is published with the understanding that IEEE and the C63 Committee members are supplying information through this Work, not attempting to render engineering or other professional services. If such services are required, the assistance of an appropriate professional should be sought. IEEE is not responsible for the statements and opinions advanced in this Work.

TABLE OF CONTENTS

DISCUSSION ON MEASUREMENT TEST DISTANCE FOR DETERMINING EIRP OR TRP FOR ACTIVE ANTENNA SYSTEMS

ABSTRACT

This paper discusses general guidance and methodologies for the determination of far-field (FF) peak gain, equivalent isotropic radiated power (EIRP), and total radiated power (TRP) of active antenna systems (AAS) at ranges shorter than the classical Fraunhofer distance (FHD).

1. SCOPE

This paper is the product of a discussion in the MIMO Study Working Group responsible for the IEEE PC63.26 draft standard on testing of transmitters used in licensed services. One topic that needs to be addressed is to determine the adequate measurement distance for the purpose of compliance demonstration of devices including antennas and antenna arrays. This paper focuses on measurements of the EIRP and TRP for intentional radiators, with particular considerations on AAS, where the antennas and transceivers are integrated, and no antenna ports can be accessed. Nevertheless, the concepts and methodologies detailed herein are also applicable when a radiofrequency port is accessible and for other quantities of interest such as the gain, directivity, and half-power beamwidth (HPBW), as defined by the IEEE Std 145™-2013 [1].[1] Although the testing of wireless devices as per IEEE Std C63.10™-2020 or draft 2 of IEEE PC63.26 requires evaluations at specific test distances, guidance on how to reduce the measurement range length and still yield acceptable measurement accuracy can be expanded in the standards. Procedures to practically increase the measurement accuracy in test sites with limited range lengths are also unavailable. Another challenge is the qualification and mitigation of uncertainty contributions in such measurements.

This paper aims to respond to the specified challenges by providing a revision of state-of-the-art far-field (FF) assessment, through the definition of an effective FF range length that is shorter than the FHD yet appropriate to derive the quantities of interest with a given certainty. It also provides brief insight into major measurement uncertainty contributions at such distances, as well as methods to characterize and mitigate them.

2. GENERAL DISCUSSION ON ACTIVE ANTENNAS

AAS with integrated antenna modules and operation at higher frequencies, such as mm-wave and sub-THz, are two major trends in the mobile industry. Such antenna systems are designed to adapt to the environment by using steerable antenna radiation patterns (i.e., beams). The number of possible beam configurations can be large. Because of this and the dynamic beamforming capabilities of devices, achieving a complete test coverage is challenging. Moreover, the lack of connectors between the radio and the antenna has led to the merging of transceiver and antenna testing. For example, transceiver parameters such as ACLR, EVM, OOBEs, and spurious emissions are tested OTA. Furthermore, the absence of antenna ports has led to conducted power being replaced by TRP.

[1] Numbers in brackets correspond to the list of sources in Section 7.

When evaluating the AAS transmitter characteristics, the basic parameter to be measured is the EIRP. This parameter reflects the capability of the AAS to concentrate power in a certain direction and is mathematically defined as a limit toward infinite distance. A finite test distance is used for practical measurements. The choice of this distance is critical, as it signifies a trade-off point between characterization accuracy and the size/cost of the test facility. To meet the demand for higher data rates, AASs tend to be electrically larger and operate at higher frequencies. Similarly, the required measurement distance in OTA test sites potentially increases beyond the available test chamber dimensions. In such situations, tests cannot be conducted by following established guidelines. This topic is explored further in the Section 3.

3. FAR-FIELD DISTANCE DISCUSSION

3.1. EFFECTIVE FAR-FIELD DISTANCE

The FF region is where the angular distribution of the field radiated by an antenna is essentially independent of the distance from a specified point in the antenna's region (IEEE Std 145-2013 [1]). Under such conditions, the electric (**E**) and magnetic (**H**) field vectors are transverse to the direction of propagation and considered to be well approximated by their asymptotic forms, such as

$$\mathbf{E}\,(R,\theta,\varphi) = \frac{e^{jkR}}{kR}\boldsymbol{F}(\theta,\varphi) \tag{1}$$

$$\mathbf{H}\,(R,\theta,\varphi) = \frac{1}{Z_0}\mathbf{k}\times\mathbf{E}\,(R,\theta,\varphi) \tag{2}$$

where (R,θ,φ) refers to standard spherical coordinates, and $\boldsymbol{F}(\theta,\varphi)$ is the vector FF radiation pattern. In the above formulas, an $e^{-j\omega t}$ time-dependence is assumed, where $\omega = 2\pi f$ is the angular frequency of the field and f is the carrier frequency of the signal. The origin of the coordinate system is typically chosen at a particular DUT reference point, such as the center of its antenna aperture or its radiation center. These terms and choice of the reference point are further discussed in Section 4. The variable R represents the distance from the observation point to the electromagnetic source and is usually called "range length," when it defines the distance to the physical measurement antenna at the test site. The angles of observation θ, φ are also called elevation and azimuth. $Z_0 = 120\pi\ \Omega$ stands for the free-space wave impedance. $\mathbf{k} = k\,\mathbf{u}_r$ is the wave propagation vector, where $k = 2\pi/\lambda$ with λ being the free-space wavelength and $\mathbf{u}_r$ is the unit radial vector. Figure 1 depicts these parameters.

FIGURE 1 **Illustration of the involved parameters**

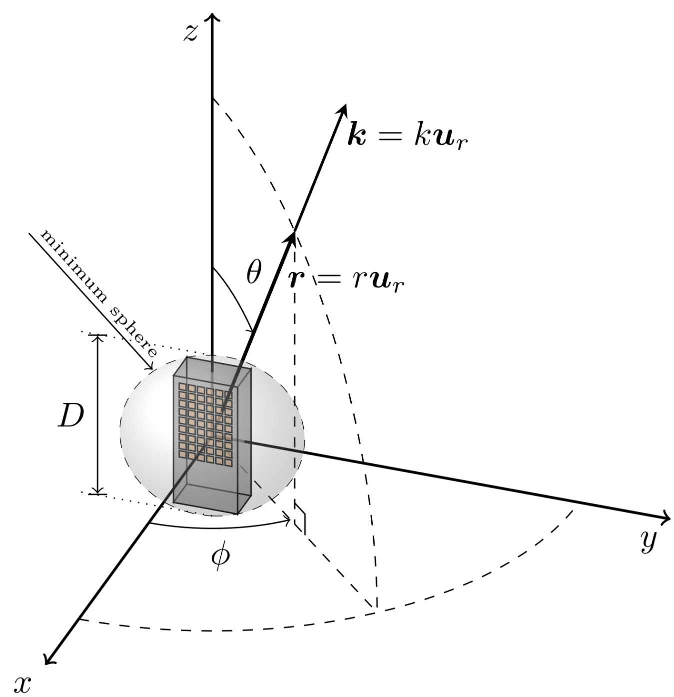

In practice, the FHD is used as the distance at which the FF condition starts. The FHD is defined by Equation (3):

$$\text{FHD} = \frac{2D^2}{\lambda} \tag{3}$$

where *D* is the diameter of the radiating source.

Without a priori knowledge of the DUT, *D* can be chosen to be the diameter of the minimum sphere encompassing the DUT. Consequently, in a direct FF probing approach, it is usually considered that the measurement range length *R* needs to be greater than or equal to the FHD, to yield acceptable accuracy (IEEE Std 149-2021 [2]). More precisely, the FHD is defined as the distance at which the sources that are confined in a region with diameter *D* create a maximum phase error of $\pi/8$ in the FF radiation pattern (Selvan and Janaswamy [3]). Ensuring a limited phase variation of the electromagnetic field incoming at the test antenna is necessary to guarantee an accurate evaluation in low-power areas of the radiation pattern, including side lobes and nulls (IEEE Std 145-2013 [1]). Yet, the FHD overestimates the required test distance, when only the power at or near the peak of radiation is of interest (peak EIRP), or for measuring spherically integrated quantities such as the TRP. This fact is demonstrated in and publication by Derat [4], which also defines a practical condition to conduct an accurate FF peak measurement. This result is derived from the analysis of physical limitations of antennas in terms of maximum achievable power gain to quality factor ratio(Geyi [5]), and the minimum number of spherical modes or harmonics required to approach this bound (Hansen [6]) by a maximum tolerated deviation of ε. Those lower radial-order modes are the ones dominantly contributing to the peak power gain. Understandably, a range length ensuring a near-asymptotic behavior of these relevant modes results in an electromagnetic field satisfying Equation (1) and Equation (2), providing sufficient conditions to measure a peak EIRP with the maximum allowed tolerance ε. The general formula for this EFFD (ε) was identified and validated in Derat [4], [7] for ε = 0.5 dB.

$$\text{EFFD } (\varepsilon = 0.5 \text{ dB}) = \lambda \left(\frac{\pi D}{\lambda}\right)^{0.8633} \left[0.1673 \left(\frac{\pi D}{\lambda}\right)^{0.8633} + 0.1632\right] \quad (4)$$

Baggett [8] provides an independent confirmation of this formula. IEC/IEEE 63195-1:2022 [9] also delivers a validation of this formula in its Annex H, demonstrating its applicability as a "far-field boundary" for incident power density measurements used to establish compliance of wireless devices to applicable human exposure limits, for devices transmitting from 6 to 300 GHz. Yuffa, *et al.* [10] provides an extension allowing calculation of the EFFD for arbitrary ε for D ranging from 3λ to more than 300λ. The spherical harmonics have well-known radial and angular dependencies. For a mode of radial order n, the variations as a function of R are expressed in terms of the spherical Hankel function of the second kind of order n, as well as its first derivative. Abramowitz and Stegun [11] provided the spatial cut-off inequality, defining the distance at which a Hankel function of order n behaves essentially like its asymptotic form in $1/R$ [as in Equation (1) and Equation (2)].

$$kR \geq n(n+1) \quad (5)$$

From Yuffa, *et al.* [10], the maximum radial order $n_{\max}$ to consider for achieving the stated accuracy ε in the peak radiation can be derived as

$$n_{\max} = \left(\frac{kD}{2}\right)^{\beta} + \alpha \left(\frac{kD}{2}\right)^{1/3} + 2 \quad (6)$$

where α and β are functions of ε. From the method proposed in Yuffa, *et al.* [10], these functions are computed for ε varying from 1% to 40%, which corresponds to a maximum error from ±0.04 to ±2.24 dB on the peak EIRP. Table 1 lists the computed values.

TABLE 1 α and β as functions of the maximum allowed deviation ε to FF in %, computed from the algorithms of Yuffa, et al. [10]

ε (%)	max $\lvert\varepsilon\rvert$ (dB)	α	β	ε (%)	max $\lvert\varepsilon\rvert$ (dB)	α	β
1	0.04	0.619	0.9851	21	1.02	−0.537	0.7744
2	0.09	0.369	0.9722	22	1.08	−0.538	0.7646
3	0.13	0.192	0.9601	23	1.14	−0.539	0.7548
4	0.18	0.055	0.9485	24	1.19	−0.539	0.7451
5	0.22	−0.055	0.9373	25	1.25	−0.539	0.7353
6	0.27	−0.146	0.9263	26	1.31	−0.538	0.7256
7	0.32	−0.219	0.9156	27	1.37	−0.537	0.7159
8	0.36	−0.281	0.9050	28	1.43	−0.536	0.7063
9	0.41	−0.332	0.8946	29	1.49	−0.534	0.6966
10	0.46	−0.374	0.8843	30	1.55	−0.532	0.6870
11	0.51	−0.409	0.8740	31	1.61	−0.530	0.6774
12	0.56	−0.437	0.8639	32	1.67	−0.528	0.6678
13	0.60	−0.462	0.8538	33	1.74	−0.528	0.6583
14	0.66	−0.480	0.8437	34	1.80	−0.527	0.6488
15	0.71	−0.495	0.8337	35	1.87	−0.524	0.6393
16	0.76	−0.508	0.8237	36	1.94	−0.525	0.6299
17	0.81	−0.517	0.8138	37	2.01	−0.523	0.6204
18	0.86	−0.525	0.8039	38	2.08	−0.524	0.6111
19	0.92	−0.531	0.7940	39	2.15	−0.522	0.6017
20	0.97	−0.535	0.7842	40	2.22	−0.522	0.5924

The following approximate explicit relations for α and β are obtained by applying least-square fitting on the computed values:

$$\alpha(\varepsilon) = -0.6094e^{-0.004075\varepsilon} + 1.433e^{-0.1934\varepsilon} \tag{7}$$

$$\beta(\varepsilon) = +0.00003867\varepsilon^2 - 0.01164\varepsilon + 1 \tag{8}$$

These functions are represented in Figure 2.

FIGURE 2 ***α*** **and** ***β*** **as functions of the maximum allowed deviation** ***ε*** **to FF in %, with least-square fits**

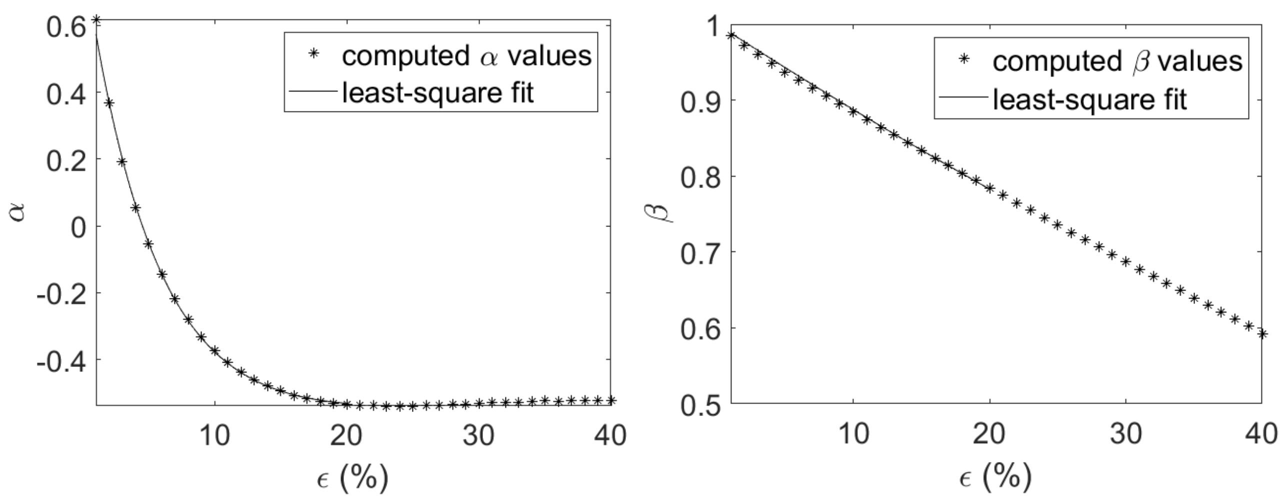

The generalized EFFD, for arbitrary error values ε, can be calculated by combining Equation (5) and Equation (8). Considering a wavelength-normalized EFFD, EFFDN = EFFD/λ, then the relation in Equation (9) holds:

$$\text{EFFDN}\left(\varepsilon, \frac{D}{\lambda}\right) = \frac{1}{2\pi} n_{\max}(n_{\max} + 1) \tag{9}$$

Figure 3 shows the ratio of the EFFD over the FHD as a function of ε in % and D/λ. The figure visualizes that the EFFD is less than 50% of the FHD for $D/\lambda \geq 3$ when a maximum EIRP error of 20% is allowed. The EFFD gets closer to the FHD when a small deviation is imposed and as D/λ decreases.

FIGURE 3 **EFFD/FHD as a function of allowed FF error** ***ε*** **and** ***D*****/λ**

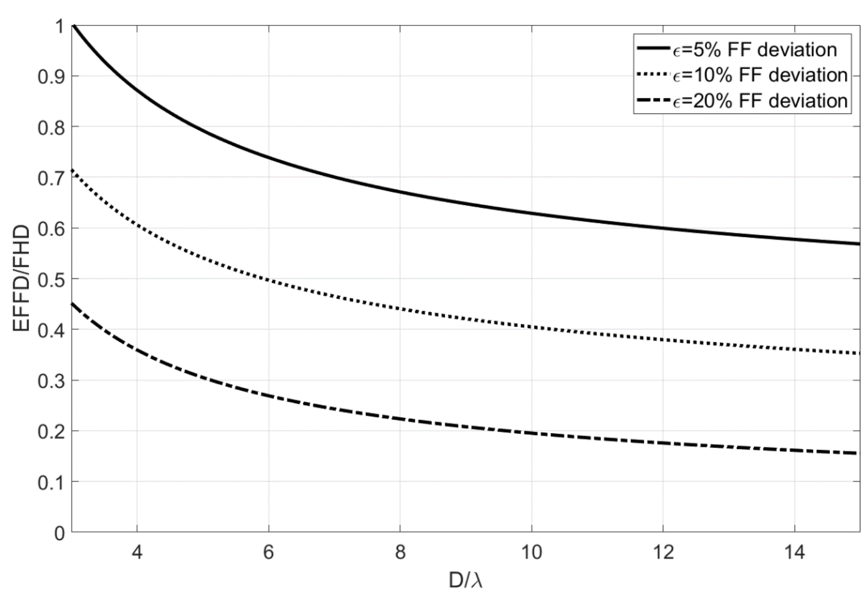

Based on Equation (9), Figure 4 exhibits the EFFDN as a function of D/λ and the maximum tolerated error ε in %, represented by isolines. The EFFDN is the minimum range length to wavelength ratio R/λ, which guarantees an error on the EIRP measurement of less than ε. An (EFFDN, D/λ)-point on the left side of an ε %-isocurve, hence, denotes that if R/λ is more than this EFFDN, then an FF characterization of the device with D/λ electrical radiation aperture size or less can be realized with better than ε % error.[2]

FIGURE 4 EFFDN as a function of allowed FF error ε and D/λ

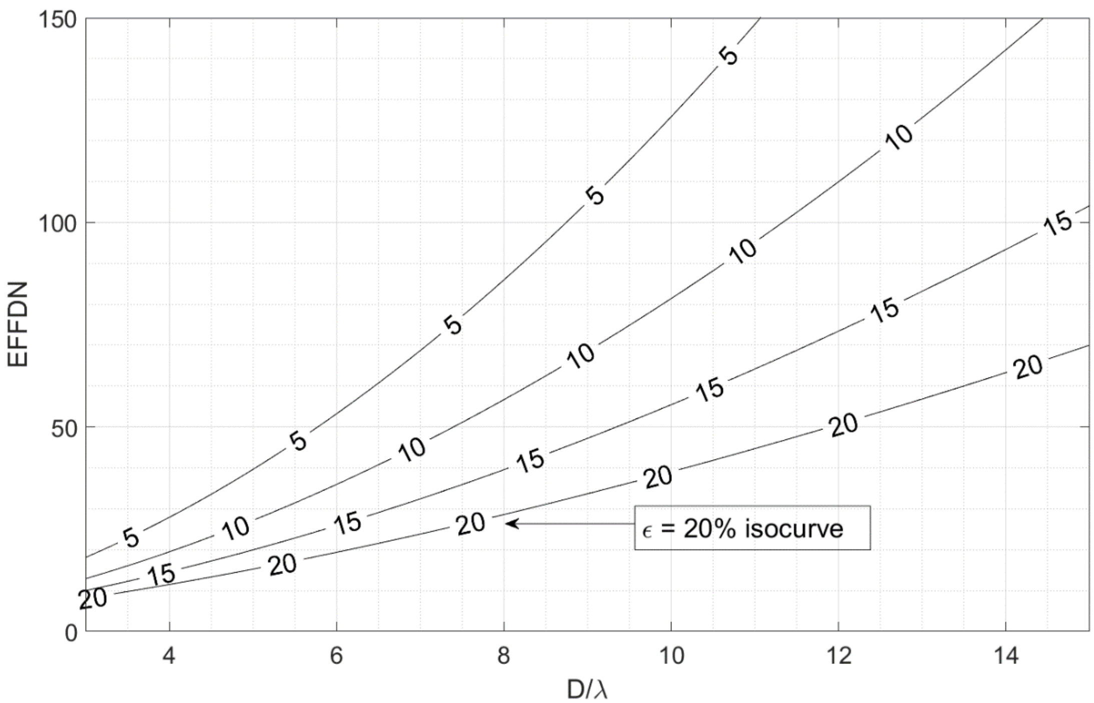

Figure 5 and Figure 6 present an alternative look at the previous equations. Supposing an anechoic chamber of fixed dimension with 3 m (Figure 5) or 10 m (Figure 6) range length, the isocurves represent the boundaries where any device operating at a frequency (f) and with a radiation aperture (D), such that the point (f, D) is on the right side of the isoline is likely to exhibit an FF measurement error greater than the indicated value on the curve. On the contrary, for a point on the left side, the iso-value gives a majorant of the expected deviation from FF.

[2] This error does not account for uncertainties relating to measurement instrumentation and DUT.

FIGURE 5 **FF error boundaries (isolines) as a function of DUT radiation aperture (cm) and frequency (GHz) for a chamber with a 3 m range length**

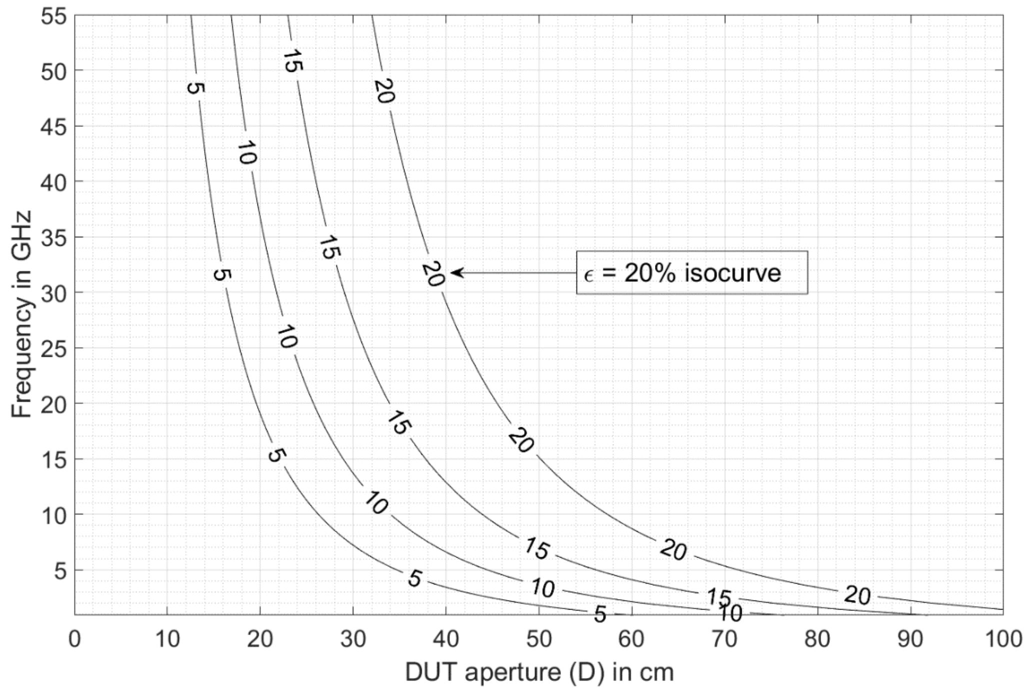

FIGURE 6 **FF error boundaries (isolines) as a function of DUT radiation aperture (cm) and frequency (GHz) for a chamber with a 10 m range length**

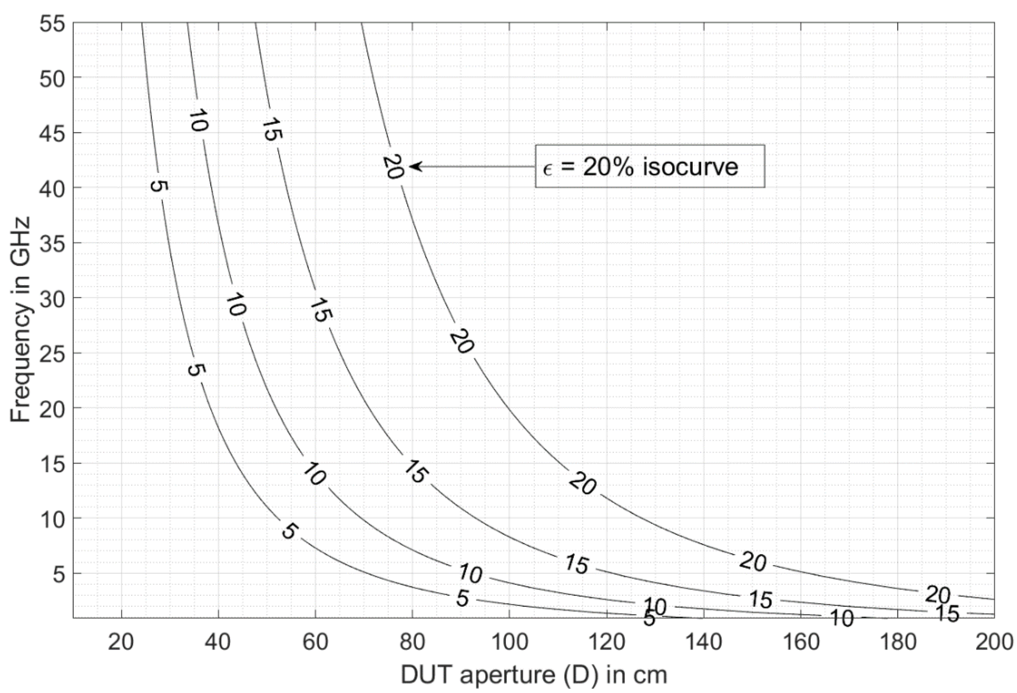

3.2. APPLICABILITY OF THE EFFD TO ANTENNA ARRAYS

In Derat, *et al*. [12] and El Hajj, *et al.* [13], studying the specific case of planar antenna arrays, the actual range length providing 0.5 dB peak directivity error was found to be shorter by a factor of 1.5 or more compared to EFFD (ε = 0.5 dB) [Equation (1)]. Derat, *et al.* [12] provided an interpretation of why this result generally holds for planar antenna arrays, with the corollary that the EFFD/FHD in the peak will decrease with the number of elements in the array. For array antennas, El Hajj, *et al.* [13] demonstrated that the EFFD (ε = 0.5 dB) also overestimates the necessary range length for HPBW, as well as for EIRP in directions of radiation 9 dB below the peak.

3.3. INFLUENCE OF BEAM-STEERING

Through simulations of planar patch arrays, El Hajj *et al.* [13] demonstrated that the EFFD is essentially not influenced by the steering of the pattern. This means, in practice, that FF assessment at or around the beam peak for a given antenna array can be carried out at the same distance and with similar accuracy for different beams.

This can be further justified from Equation (11) in Derat, *et al.* [12], which uses the plane-wave spectrum (*k* or wavenumber-space) formalism (Kern and Daly [14]) to describe the radiation from an arbitrary antenna array, based on the field from its elements. The steering of the array beam introduces a translation in the *k*-space of the spectral array factor function. This can be intuitively interpreted by the idea that the field radiated by the array in the direction of the peak of the steered beam is obtained from a constructive interference (obtained via the tuning of the array excitation coefficients) of the fields from its constitutive elements, in the same direction of observation. One can assume that arrays are nominally used with steering angle directions at which the constitutive elements provide efficient radiation. In these directions and based on results discussed in Section 3.2, the EFFD of the element is expected to be similar to in the boresight direction. As a result, the array field, which is the linear combination of the fields from all elements, will also show similar FF convergence properties compared to boresight.

3.4. TRP MEASUREMENT DISTANCE CONSIDERATIONS

TRP measurements can be carried out at even shorter distances than the EFFD because, in free space, the TRP going through a sphere encompassing the DUT is independent from the radius of the sphere (Derat, *et al.* [7], Friden, *et al.* [15]). It is, however, important to note that, as the measurement antenna and scanning schemes are nonideal, error contributors are possibly degrading the accuracy of measurements at shorter range lengths for the TRP as well. A significant contribution to the uncertainty is related to the offset of center-of-phase from the coordinate system (Hamberger, *et al.* [16]). It is also demonstrated that this contribution can be compensated by post-processing.

4. MEASUREMENT ASPECTS AND UNCERTAINTY

4.1. EXPERIMENTAL VALIDATION OF FAR-FIELD CONDITION

It is possible to experimentally estimate an EFFD, directly from FF approximate power density measurements at various distances.[3] If the FF approximate power density $P_D(R) = |\mathbf{E}|^2/2Z_0$ decays as $1/R^2$ along the same angular direction, then an FF condition has been practically reached (Moogilan [17]). This is identified as a constant level of the EIRP estimate $\mathrm{EIRP}_{\mathrm{est},}$ via the relation in Equation (10).

$$\mathrm{EIRP}_{\mathrm{est}} = 4\pi R^2 P_D(R) \tag{10}$$

The proper reference points for the test antenna and the DUT used to calculate the distance *R* have an impact on the accuracy of the EIRP estimate as the distance decreases. An investigation of this topic in the case of determining the realized gain can be found in two papers by van den Biggelaar ([18] and [19]), which propose to use the amplitude center of the antenna in contrast to the widely used phase center or center of the antenna aperture as a reference point. Note also that the phase center for most antenna types varies with frequency. Moreover, its definition [1] is ambiguous and can lead to different results in different numerical implementations of algorithms to evaluate the phase center location. A remedy to this can be found in Fridén and Kristensson [20] where a radiation center is defined and proven to be unique for any antenna. The calculation of the radiation center, as defined in Fridén and Kristensson [20], however requires that electric or magnetic field data are characterized over a full sphere, for two orthogonal polarizations, and in magnitude and phase. In general, a

[3] The power density generally expresses as the real part of the Poynting vector at a given point in space. It is only in the FF that the power density can be rigorously expressed as $|\mathbf{E}|^2/2Z_0$.

careful choice of the reference point may allow for measuring at closer distances by minimizing the effective diameter *D*, in the previous formulas (Section 3.1).

4.2. EVALUATING FAR-FIELD PARAMETERS FROM NEAR-FIELD MEASUREMENTS[4]

When the available range length at a given site is shorter than the EFFD, which could support a target accuracy as defined in Section 3, direct FF measurements are no longer possible. Alternatives do exist that enable the evaluation of FF parameters from near-field measurements so that the site could still be utilized. A multiplicity of near-field antenna characterization techniques, coupled with near-field to FF transformations are known and largely documented in IEEE Std 1720™-2012 [21] and Parini, *et al.* [22] and [23]. However, such methods involve the measurement of the magnitude and phase of components of the electromagnetic field, typically obtained from transmission *S*-parameter measurements. Phaseless approaches can also be applied, which are used to retrieve phase information from additional field amplitude measurements. Vector network analyzer measurements or traditional phaseless techniques are not generally applicable to the characterization of self-powered transmitting devices using digitally modulated signals, and where no RF connector is typically available. Derat, *et al.* [24], [25] describe a way to extract the electromagnetic propagation phase information that applies to such a situation and requires the use of a two-port phase-coherent signal analyzer. One of these ports is then used to connect the measurement antenna, while the other one is linked to a reference antenna fixed with respect to the DUT. As the modulation phase variations affect both signals in the same way, the phase difference between the two measured signals eliminates the influence of the modulation and enables the isolation of the relevant phase information.

Another alternative or the so-called extrapolation technique was originally published in Newell, *et al.* [26] and further clarified in Yuffa [27]. It is demonstrated that the signal received by the measurement antenna, illuminated by the field from the transmitting DUT, can be expanded in a weighted sum of powers of $1/R$. From on-axis magnitude measurements at various distances, the data can be fitted to such a series summation, including all terms of relevant orders. The fitting particularly allows the evaluation of the coefficient of the $1/R$ term, which provides the target FF information.[5]

[4] This section is for informational purposes and not a detailed discussion on near field measurements.
[5] Informational purposes only—not a detailed discussion of the topic. See the references cited in this section for more information.

4.3. MEASUREMENT UNCERTAINTY CONSIDERATIONS

This section provides an overview of uncertainty terms that specifically affect the measurements of FF quantities at short-range lengths. Neither an uncertainty model nor detailed methodologies to assess these various contributors are described hereafter. General aspects relating to measurement uncertainty can be found in *Evaluation of Measurement Data* [28], and more specifically for antenna measurements in IEEE Std 149-2021 [2]. subclause B.3.1 of 3GPP TR 38.903 [29] contains a description of components that contribute to EIRP and TRP measurement uncertainty in a direct FF assessment setup (not involving a near-to-FF software transformation, or hardware transformation using, e.g., a compact antenna test range).

4.3.1. RANGE ANTENNA ALIGNMENT/POSITIONING

The positioning tolerance of the range antenna introduces errors in the measurement of the total EIRP and the EIRP of individual field components. The contribution differs depending on the displacement along the measurement axis (radial direction in spherical measurements), or transverse to the measurement axis. If the misalignment is fixed for all measurement angles, this creates biases for which compensation approaches may be applied. If such displacements vary with the angular position, then this can be accounted for as a component of the overall measurement uncertainty.

For a given absolute mechanical error, the actual influence on uncertainty at shorter measurement distances is inflated, as this absolute deviation represents a larger relative deviation with respect to the range length. For example, as per Equation (10), the EIRP estimate is obtained as a product of $4\pi R^2$ to the power density. In the first order, a positioning error dR along the axis results in a relative total EIRP deviation of $2dR/R$.

4.3.2. VARIATION OF DUT-RADIATED FIELDS ACROSS THE RANGE ANTENNA APERTURE

When measuring at closer distances, the choice of the test antenna is more elaborate than when measuring at larger distances. In particular, the beam of the test antenna will ideally illuminate the DUT as uniformly as possible. On the other hand, an overly wide beam illuminating the sidewalls and other areas of the chamber will result in higher sensitivity to scattering within the test environment. Consideration of measurement accuracy is hence important when selecting the antenna. A pragmatic rule of thumb is that the HPBW of the test antenna shall cover the DUT (IEEE Std 149-2021 [2]). By reciprocity, the HPBW criterion helps to ensure that the field of the DUT is uniform enough over the test antenna aperture (Fridén, *et al*. [15]).

4.3.3. DUT RADIATION CENTER OFFSET FROM CENTER OF COORDINATES

As the measurement antenna scans the test surface, three major aspects affect the measured radiation pattern accuracy, when the DUT center of phase is offset from the center of the system coordinates. They are as follows:

(1) The propagation path length varies across the scanned surface, giving rise to additional phase variations in the measured field.

(2) The DUT radiation center angular position, taken in a local coordinate system attached to the probe, changes with the probe location in the measurement coordinate system. Consequently, it may not be accurate enough to consider a constant gain value for the measurement probe.

(3) The grid of sampled points does not coincide with the desired measurement grid, which would ideally be used for EIRP captures if the DUT were centered.

As demonstrated in Hamberger, *et al*.[16], these various points may contribute to errors in the EIRP and TRP. The impact is even more pronounced at short-range lengths, as the displacement from the center of measurement coordinates becomes relatively larger. Hamberger, *et al*. [16] provides an algorithm to compensate for the related deviations. This method works for both transmit and receive modes of the DUT and requires no electromagnetic field phasor measurements. The main assumptions for the applicability of this technique are that the DUT radiation center position is known (or can be reasonably approximated by the mechanical center of the radiation portion of the DUT) and that the minimum antenna to DUT distance at all measurement positions is higher than the applicable EFFD. In this case, (1)–(3) can be mitigated, respectively, by: (i) performing a geometrical correction of the path length; (ii) adapting the antenna gain at each measurement location using its gain pattern data in the direction of the DUT phase center; and (iii) realizing an interpolation to evaluate the EIRP at the target sampling grid.

4.3.4. SPHERICAL GRID ANGULAR SAMPLING

The relation between angular sampling of the field and pattern measurement accuracy is known and well documented in Fridén, *et al*. [15] for TRP. For TRP measurements, coarser sampling rates can be applied provided that appropriate averaging algorithms are used.[6] It is important to note that the error related to the limited sampling rate can be correlated with other uncertainty components, such as the DUT radiation center offset from the center of coordinates (see 4.3.3).

[6] A known algorithm providing a robust average with a relatively small number of points is the Clenshaw–Curtis quadrature integral approximation [30].

4.3.5. STANDING WAVE BETWEEN DUT AND RANGE ANTENNA

Standing waves might form between the DUT and the test antenna. The standing wave effect can be detected by slightly varying the test distance. To reduce this effect, a low scattering antenna such as an open-ended waveguide can be used. Furthermore, the standing wave ripple can be filtered out from the measurement data by taking samples at multiple distances (Newell, et al. [26]).

5. ADDITIONAL CONSIDERATIONS

5.1. UNWANTED EMISSIONS

OOB and spurious emissions, though affected by antenna gain, are tested at fixed distances per the test standard or regulation. Aside from knowing the overall maximum gain, unwanted emissions do not play a factor in this measurement discussion.

5.2. BEAM-STEERING

Test methodologies for active antennas can be divided into categories based on their objective. “Worst-case” metrics are desired in some cases, where one may be interested in the maximum EIRP or the maximum gain. In other cases, one may be interested in measurements of individual beams from a multibeam antenna array. In this section, some of the available test methods for these two broad categories of objectives will be addressed.

The boresighting issue needs to be brought into the discussion. Usually, the worst-case mode is when all array elements are steered in the same location. Boresight radiation, which is ideally obtained by in-phase excitation of the antenna array elements, generally delivers the highest EIRP.

In regard to testing, it may be more relevant to test the manufacturers’ predetermined combinations than trying to determine the worst-case mode without their input.

An increasingly important consideration in the testing of active array systems is the number of array beam states that need to be measured. As active array systems become increasingly complex, it becomes more impractical to measure characteristics from every state. The exact point at which the number of states makes testing impractical is debatable. Beyond this point, one can utilize a variety of tools to help make informed decisions about which beam states to test. The selection of beam states to test may be based on policy (e.g., maximum gain), application (e.g., typical number of beams), or statistical analysis. The development of a procedure for boresighting should be considered as a topic of discussion.

6. CONCLUSION/FURTHER QUESTIONS

The guidance provided in this paper is intended to be used when developing measurement standards and should help with addressing some of the issues to better facilitate the testing of AASs on various sites and chambers. It provides a way to determine the maximum antenna aperture size that can be tested in the FF at a given frequency and for a maximum error in an existing chamber with a defined range length. Furthermore, it also describes an approach to evaluate the minimum range length required to perform an FF assessment for an antenna of a given aperture and at a given frequency, with a maximum acceptable deviation to ideal FF.

7. REFERENCES

The following sources have either been referenced within this paper or may be useful for additional reading:

[1] IEEE Std 145™-2013, *IEEE Standard for Definitions of Terms for Antennas*, Mar. 6, 2014, pp. 1–50, doi: 10.1109/IEEESTD.2014.6758443.

[2] IEEE Std 149™-2021, *IEEE Recommended Practice for Antenna Measurements*, Feb. 18, 2022, doi: 10.1109/IEEESTD.2022.9714428.

[3] K. T. Selvan and R. Janaswamy, “Fraunhofer and Fresnel distances: Unified derivation for aperture antennas,” *IEEE Antennas Propag. Mag.*, vol. 59, no. 4, pp. 12–15, Aug. 2017.

[4] B. Derat, “5G antenna characterization in the far-field: How close can far-field be?” in *Proc. Int. Symp. Electromagn. Compat. (APEMC)*, May 2018, pp. 959–962.

[5] W. Geyi, “Physical limitations of antenna,” *IEEE Trans. Antennas Propag.*, vol. 51, no. 8, pp. 2116–2123, Aug. 2003, doi: 10.1109/TAP.2003.814754.

[6] J. E. Hansen, *Spherical Near-Field Antenna Measurements* (Electromagnetic Waves). London, U.K.: The Institution of Engineering and Technology, 1988.

[7] B. Derat, G. F. Hamberger, and F. Michaelsen, “Shortest range length to measure the total radiated power,” *IET Microw., Antennas Propag.*, vol. 13, no. 15, pp. 2584–2589, Dec. 2019.

[8] M. Baggett, “A trade study on quasi far-field accuracies and measurements,” in *Proc. Antenna Meas. Techn. Assoc. Symp. (AMTA)*, Denver, CO, USA, Oct. 2022, pp. 1–6, doi: 10.23919/AMTA55213.2022.9954603.

[9] IEC/IEEE 63195-1, *IEC/IEEE International Standard—Assessment of Power Density of Human Exposure to Radio Frequency Fields from Wireless Devices in Close Proximity to the Head and Body (Frequency Range of 6 GHz to 300 GHz)—Part 1: Measurement Procedure*, May 10, 2022, doi: 10.1109/IEEESTD.2022.9770427.

[10] A. J. Yuffa, M. A. Valdez, and B. Derat, "On Convergence of the upper bound on the ratio of gain to quality factor," in *Proc. Antenna Meas. Techn. Assoc. Symp. (AMTA)*, Oct. 2021, pp. 1–3.

[11] M. Abramowitz and I. Stegun, *Handbook of Mathematical Functions*. Mineola, NY, USA: Dover, 1964, p. 364.

[12] B. Derat et al., "Validation of over-the-air testing accuracy at mid-range distance for massive MIMO base stations," in *Proc. Antenna Meas. Techn. Assoc. Symp. (AMTA)*, Oct. 2021, pp. 1–6.

[13] W. El Hajj et al., "Practical and empirical measurement distance definition for 5G devices at mm-waves," in *Proc. IEEE Conf. Antenna Meas. Appl. (CAMA)*, Nov. 2021, pp. 357–362.

[14] D. M. Kerns and P. W. Daly, "Plane-wave scattering matrix theory of antennas and antenna-antenna interactions," National Bureau of Standards Monograph, Gaithersburg, MD, USA, Tech. Rep. NBS 162, 1981.

[15] J. Fridén, A. Razavi, and A. Stjernman, "Angular sampling, test signal, and near-field aspects for over-the-air total radiated power assessment in anechoic chambers," *IEEE Access*, vol. 6, pp. 57826–57839, 2018.

[16] G. F. Hamberger, et al., "Correction of over-the-air transmit and receive wireless device performance errors due to displaced antenna positions in the measurement coordinate system," *IEEE Trans. Antennas Propag.*, vol. 68, no. 11, pp. 7549–7554, Jun. 2020.

[17] D. Moogilan, "Wireless MIMO base station near and far field measurement challenges," in *Proc. IEEE Int. Symp. Electromagn. Compat. Signal/Power Integrity (EMCSI)*, Aug. 2017, pp. 543–548.

[18] A. J. van den Biggelaar et al., "Accurate gain measurement technique for limited antenna separations," *IEEE Trans. Antennas Propag.*, vol. 69, no. 10, pp. 6772–6782, Oct. 2021, doi: 10.1109/TAP.2021.3069583.

[19] A. J. van den Biggelaar, A. B. Smolders, and U. Johannsen, "Method to experimentally verify far-field conditions in a direct far-field measurement setup," in *Proc. Antenna Meas. Techn. Assoc. Symp. (AMTA)*, Oct. 2021, pp. 1–6.

[20] J. Fridén and G. Kristensson, "Calculation of antenna radiation center using angular momentum," *IEEE Trans. Antennas Propag.*, vol. 61, no. 12, pp. 5923–5930, Dec. 2013, doi: 10.1109/TAP.2013.2283033.

[21] IEEE Std 1720-2012, *IEEE Recommended Practice for Near-Field Antenna Measurements*, pp. 1–102, Dec. 5, 2012, doi: 10.1109/IEEESTD.2012.6375745.

[22] C. Parini et al., *Theory and Practice of Modern Antenna Range Measurements* (Electromagnetic Waves). London, U.K.: IET Digital Library, 2014. [Online]. Available: https://digital-library.theiet.org/content/books/ew/pbew055e

[23] C. Parini et al., *Theory and Practice of Modern Antenna Range Measurements* (Electromagnetic Waves), vol. 2, 2nd ed. London, U.K.: IET Digital Library, 2020. [Online]. Available: https://digital-library.theiet.org/content/books/ew/sbra538g

[24] B. Derat et al., “Base station specific absorption rate assessment based on a combination of over-the-air measurements and full-wave electromagnetic simulations,” in *Proc. Antenna Meas. Techn. Assoc. Symp. (AMTA)*, Oct. 2021, pp. 1–6, doi: 10.23919/AMTA52830.2021.9620622.

[25] B. Derat, M. Erkocevic, and G. F. Hamberger, “Reconstruction of near-field millimeter-wave power density from over-the-air measurements,” in *Proc. IEEE Conf. Antenna Meas. Appl. (CAMA)*, Nov. 2021, pp. 306–310, doi: 10.1109/CAMA49227.2021.9703486.

[26] A. Newell, R. Baird, and P. Wacker, “Accurate measurement of antenna gain and polarization at reduced distances by an extrapolation technique,” *IEEE Trans. Antennas Propag.*, vol. 21, no. 4, pp. 418–431, Jul. 1973.

[27] A. J. Yuffa, “On Wacker’s essential equation in the extrapolation measurement technique,” in *Proc. Antenna Meas. Techn. Assoc. Symp. (AMTA)*, San Diego, CA, USA, Oct. 2019, pp. 1–5.

[28] *Evaluation of Measurement Data—Guide to the Expression of Uncertainty in Measurement*, document JCGM 100:2008, Sep. 2008.

[29] TR 38.903, 3rd Generation Partnership Project; Technical Specification Group Radio Access Network; NR; Derivation of test tolerances and measurement uncertainty for User Equipment (UE) conformance test cases (Release 16) version 16.11.0, Mar. 2022.

[30] C. W. Clenshaw and A. R. Curtis, “A method for numerical integration on an automatic computer,” *Numerische Mathematik*, vol. 2, pp. 197–205, Dec. 1966.

[31] P. J. Davis and P. Rabinowitz, *Methods of Numerical Integration*. San Diego, CA, USA: Academic Press, 1984.

APPENDIX A

ACRONYMS AND ABBREVIATIONS

AAS	active antenna system
ACLR	adjacent channel leakage ratio
DUT	device under test
EFFD	effective far-field distance
EIRP	equivalent isotropically radiated power
EVM	error vector magnitude
FF	far-field
FHD	Fraunhofer distance
HPBW	half-power beamwidth
IB	in-band
MIMO	multiple-input multiple-output
OOB	out of band
OOBE	out of band emission
OTA	over-the-air
TRP	total radiated power

RAISING THE WORLD'S STANDARDS

3 Park Avenue, New York, NY 10016-5997 USA http://standards.ieee.org

Tel. +1 732-981-0060 Fax +1 732-562-1571